JOURNAL OF MATERIALS SCIENCE 29 (1994) 4481–4486

Synthesis and thermal evolution of structure in alkoxide-derived niobium pentoxide gels

N. P. BANSAL
National Aeronautics and Space Administration, Lewis Research Center, Cleveland, Ohio 44135, USA

Niobium pentoxide gels in the form of transparent monoliths and powder have been synthesized from the controlled hydrolysis and polycondensation of niobium pentaethoxide under different experimental conditions using various mole ratios of $Nb(OC_2H_5)_5 : H_2O : C_2H_5OH : HCl$. Alcohol acted as the mutual solvent and HCl as the deflocculating agent. In the absence of HCl, precipitation of colloidal particles was encountered on the addition of any water to the alkoxide. The gels were subjected to various thermal treatments and characterized by differential thermal analysis, thermogravimetric analysis, X-ray diffraction and infra-red spectroscopy. After drying at 400 °C, the gels were amorphous to X-rays. The amorphous powder crystallized into the low temperature orthorhombic form of Nb_2O_5 at ~ 500 °C, which transformed irreversibly into the high temperature monoclinic α-Nb_2O_5 between 900 to 1000 °C. The kinetics of crystallization of the amorphous niobium pentoxide have been investigated by non-isothermal differential scanning calorimetry. The crystallization activation energy was determined to be 399 kJ mol^{-1}.

1. Introduction

The sol–gel technique has recently received significant attention [1] for the preparation of glasses, ceramic fibres, protective and other coatings, optical films, ultrapure monosized fine ceramic powders, composite materials, etc. The metal oxides synthesized by this method are generally amorphous. The structures and crystallization of these materials is of scientific interest, and their stability at elevated temperatures is technologically important. Metal oxides such as niobium pentoxide may find new applications in the form of reversible cathodes [2, 3], display devices [4], ferroelectric ceramics [5], and fibre coatings. However, very little attention [6] has been paid to the synthesis of these materials by the sol–gel process. The present study was undertaken with the objective of synthesizing the niobium pentoxide monolithic bodies and powder using the sol–gel technique. Another purpose was to investigate the thermal evolution of the physical and structural changes occurring in the gel.

Transparent monolithic niobium pentoxide gel bodies and powder were prepared under different experimental conditions. The gel was characterized by various techniques. The kinetics of crystallization of the amorphous gel powder have been studied by differential scanning calorimetry. The thermal evolution of various crystalline phases in this material was monitored by powder X-ray diffraction and the structural changes by infrared spectroscopy.

2. Experimental procedure

Niobium pentaethoxide, $Nb(OC_2H_5)_5$, from Alfa products and 200 proof absolute ethanol were used as-received. The quantities of various chemicals used are shown in Table I. Due to the high reactivity of niobium pentaethoxide towards moisture, it was handled inside a glove box. Required amounts of $Nb(OC_2H_5)_5$ were mixed with alcohol and the container was sealed with parafilm and taken out of the glove box. A 50% (v/v) HCl solution (prepared by mixing equal volumes of concentrated hydrochloric acid and water) was slowly added dropwise with constant stirring. A clear homogeneous solution resulted. In some cases more water was slowly added under vigorous stirring. The container was sealed with parafilm and kept at ambient conditions for gelation. Depending upon the concentrations of different reactants, several hours to many days were required for complete gelation.

The gels were dried for several days under ambient conditions. The dried gel was fired at various temperatures between 110 to 1450 °C in air in a platinum crucible. Thermal evolution of the gel after various heat treatments was monitored by several techniques. Differential thermal analysis (DTA) and thermogravimetric analysis (TGA) were carried out using Perkin–Elmer DTA-1700 and TGS-2 systems, respectively, which were interfaced with computerized data acquisition and analysis systems. Infrared (i.r.) transmission spectra were recorded from 4000 to 450 cm^{-1} using the KBr pellet technique with a Perkin–Elmer 1750 infrared Fourier transform spectrometer, interfaced with a Perkin–Elmer 7300 professional computer. Powder X-ray diffraction (XRD) patterns were collected at room temperature using a step-scan procedure (0.03° 2θ step; count time 0.5 s)

0022–2461

TABLE I Effect of synthesis conditions on gelling time and appearance of niobium pentoxide gels

Gel no.	Amounts of various chemicals used				H_2O:alkoxide mole ratio, r	Gelling time (h)	Gel appearance
	$Nb(OC_2H_5)_5$ (g)	C_2H_5OH (ml)	50% HCl[a] (ml)	H_2O (ml)			
NB-6	5	15	0.4 + 0.1 Conc. HCl	– –	0.71	205.0	Clear, transparent
NB-1	5	15	0.4	–	0.71	205.0	Clear, transparent
NB-5	5	15	0.6	–	1.06	40.0	Clear, transparent
NB-3	5	15	0.8	–	1.41	8.5	Very slightly translucent
NB-4	5	10	0.6	–	1.06	32.0	Clear, transparent
NB-2	5	15	0.4	0.2	1.41	0.5	Transparent; some white suspension

[a] 50% (v/v) solution of concentrated HCl in water.

in the 2θ range 10–80° on a Phillips ADP-3600 automated powder diffractometer equipped with a crystal monochromator employing CuK_α radiation.

The kinetics of crystallization of the amorphous niobium pentoxide gel powder were studied by non-isothermal differential scanning calorimetry (DSC) using a Perkin–Elmer DSC-4 system interfaced with a computer. DSC thermograms were recorded using scan rates of 1–40 °C min^{-1} under flowing air. Samples were contained in sealed aluminium DSC pans.

3. Results and discussion

3.1. Gel synthesis

Niobium pentoxide gels were prepared under different experimental conditions using various mole ratios of $Nb(OC_2H_5)_5$:H_2O:C_2H_5OH:HCl as shown in Table I. C_2H_5OH acts as the mutual solvent and HCl as the deflocculating agent. In the absence of HCl, it was not possible to prepare clear sols. Precipitation of colloidal particles was encountered on the addition of any water to $Nb(OC_2H_5)_5$ due to high reactivity of the alkoxide toward water.

In all cases the gels were clear, transparent and light yellow in colour. A typical transparent monolithic dry gel sample ~ 1.2 cm in diameter is shown in Fig. 1. The time needed for gel formation decreased with increase in water:alkoxide mole ratio, r. A comparison of NB-5 and NB-4 (Table I) shows that, for the same value of r, gelation time decreased with higher concentration of water in the solution. The HCl concentration appears to have no influence on the gelling time, as seen from a comparison of the results for NB-1 and NB-6, but its presence in the solution is necessary to avoid the precipitation of niobium hydroxide on the addition of water.

A larger batch of gel was prepared using 50 g of $Nb(OC_2H_5)_5$, 150 ml C_2H_5OH and 0.5 ml of an aqueous 50% HCl (v/v) solution. The gel was allowed to dry for five weeks under ambient conditions which resulted in yellow porous pieces. It was stored in a closed container until used for further treatment and characterization, and will henceforth be referred to as "NB".

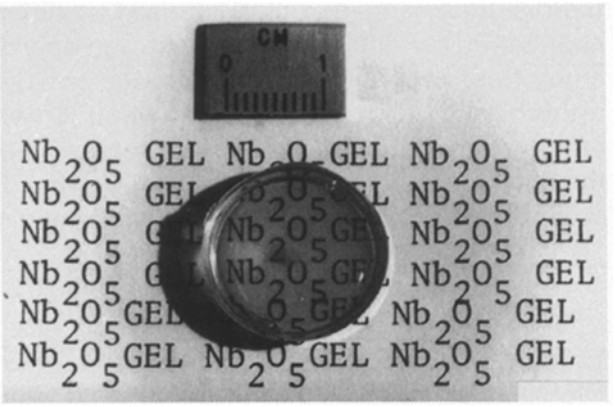

Figure 1 A typical sample of dried niobium oxide gel.

3.2. Pyrolysis of gel

The pale yellow gel "NB" was pyrolysed at various temperatures and the results are summarized in Table II. On drying at 110 °C for ~ 46 h, the gel became yellowish brown and changed to shiny metallic black after heating at 300 °C for 24 h. On further treatment at 400 °C for 24 h, it turned pale yellow. Some black particles, probably carbon, were also present due to incomplete oxidation of the organics. Up to this point the material was amorphous. On further heating at 500 °C for 24 h, the black particles disappeared. This powder was used for all further heat treatments. The powder turned shiney white after firing for 1 h at 700 or 800 °C. It became greyish white on heating at 900 °C for 1 h. When fired for 1 h at 1000, 1120 or 1300 °C the colour of the powder stayed dirty white. The powder became brownish white after heating at 1450 °C for 1 h.

3.3. X-ray diffraction

Following each thermal treatment, the samples were subjected to powder X-ray diffraction at room temperature for phase identification and average crystal size determination. The results are summarized in Table II and the typical XRD powder patterns are shown in Fig. 2. Samples A to D were amorphous to X-rays.

TABLE II Influence of thermal treatments on niobium pentoxide gel (NB)

No.	Heat treatment		Phase(s)	Grain size[a] (nm)	Comments
	Temperature (°C)	Time			
A	Ambient	5 weeks	Amorphous	–	Pale yellow
B	110	46 h	Amorphous	–	Yellowish brown
C	300	24 h	Amorphous	–	Metallic black
D	400	24 h	Amorphous		Pale yellow; some black particles
E	500[b]	24 h	Nb_2O_5[c]	35.5	Dark yellow when hot, pale yellow when cold
F	600	3 h	Nb_2O_5[c]	35.5	Light orange when hot, pale yellow when cold
G	700	1 h	Nb_2O_5[c]	37.8	Shiny white
H	800	1 h	Nb_2O_5[c]	49.0	Shiny white
I	900	1 h	Nb_2O_5[c]	51.4	Dirty white
J	1000	1 h	α-Nb_2O_5	30.8	Dirty white
K	1120	1 h	α-Nb_2O_5	35.5	Dark yellow when hot, dirty white when cold
L	1300	1 h	α-Nb_2O_5	47.0	Dark yellow when hot, dirty white when cold
M	1450	1 h	α-Nb_2O_5	69.3	Orange yellow when hot, brownish white when cold

[a] Average size evaluated from line broadening of XRD peaks.
[b] Heat treatment is cumulative up to this step; powder from this step used in all further heat treatments.
[c] J.C.P.D.S. Card No. 27–1003.

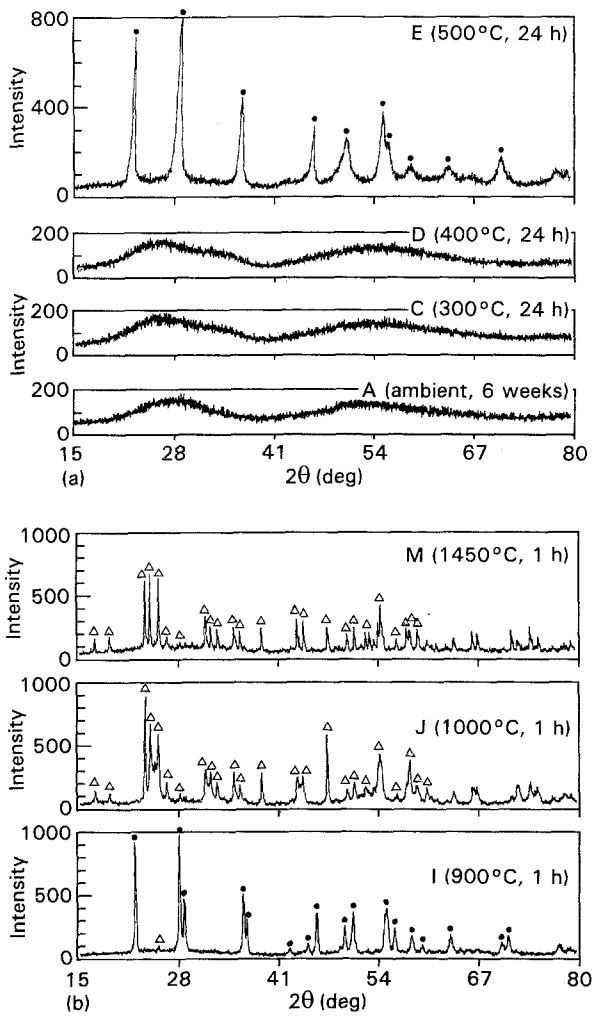

Figure 2 Powder X-ray diffraction patterns of niobium pentoxide gel samples fired at different temperatures as shown in Table II: (a) ambient to 500 °C, (b) 900–1450 °C: (○) Nb_2O_5 (No. 27–1003), (△) α-Nb_2O_5 (No. 16–53).

Two broad halos centred around 28 and 53° 2θ were present in the room temperature dried gel. On heating, the position of the former broad peak shifted to lower angles, whereas the latter peak was more or less unaffected. The presence of these broad peaks indicated the existence of short range order in these amorphous materials. The low temperature orthorhombic form [7] of Nb_2O_5 crystallized on firing at 500 °C and this phase persisted up to 900 °C (samples E to I). The amount of this crystalline phase increased with the firing temperature. The peaks at $2\theta = 28.3$ and 36.5° started to split into doublets at 700 °C and had fully developed into independent peaks at 900 °C. The (1 8 0) peak ($2\theta = 28.3°$, $d = 0.315$ nm), (2 0 0) peak ($2\theta = 28.9°$, $d = 0.309$ nm), (1 8 1) peak ($2\theta = 36.6°$, $d = 0.246$ nm) and (2 0 1) peak ($2\theta = 37.0°$, $d = 0.2428$ nm) were fully revealed in the 900 °C fired sample. The (1 8 0) peak has higher intensity than the (2 0 0) peak, and the (1 8 1) peak was more intense than the (2 0 1) peak. The low temperature orthorhombic form transformed into the high temperature monoclinic modification [8], α-Nb_2O_5, on firing between 900 to 1000 °C. This was an irreversible transformation, i.e. the α-Nb_2O_5 did not convert back into the low temperature form on cooling.

The average particle size, after each heat treatment, was estimated from X-ray line broadening analysis using the Scherrer formula

$$x = k\lambda/(B\cos\theta_B) \quad (1)$$

where x is the average particle size, $k \sim 1$, λ the wave length of CuK_α radiation, B the width (in radian) of the XRD peak at half its maximum intensity, and θ_B the Bragg diffraction angle of the line. Correction for the line broadening by the instrument was applied using a large particle size silicon standard and the

relationship

$$B_M^2 = B^2 + B_S^2 \quad (2)$$

where B_M and B_S are the measured widths, at half-maximum intensity, of the lines from the sample and the standard, respectively. The average particle size increased (Table II) with the pyrolysis temperature. The X-ray line broadening method can be used only for the size determination of small crystallites (~ 0.05 μm). Besides, the information obtained does not concern the real particle size, but the average size of coherently diffracting domains; the latter being usually much smaller than the actual size of the particles.

3.4. Thermal analyses

Thermal analyses of various gels were carried out after drying under ambient conditions. Typical DTA and TGA curves of the NB-2 gel recorded at a heating rate of 10 °C min^{-1} are presented in Figs 3 and 4, respectively. Two endothermic and two exothermic peaks are present in the DTA. The TGA shows a total weight loss of 26.7% to 950 °C, taking place in three steps. The large endothermic peak A at $\sim$ 125 °C may be attributed to the loss of residual water and alcohol entrapped in micropores of the gel. The TGA shows a substantial weight loss of $\sim$ 18.5% from room temperature to $\sim$ 220 °C (step I). The second endothermic peak B at 390 °C in the DTA, and the $\sim$ 6.4% weight loss in the temperature region 355–423 °C (step II) in TGA, may be assigned to the loss of structural water by dehydration condensation of hydroxyl groups. The exothermic peak C at $\sim$ 492 °C in the DTA, and the $\sim$ 0.5% loss of weight from $\sim$ 518–540 °C (step III) in the TGA are probably caused by oxidation of the residual organics. The exothermic peak D at $\sim$ 535 °C in the DTA is ascribed to the crystallization of the amorphous material into the low temperature orthorhombic form [7] of Nb_2O_5 as confirmed from XRD (*vide supra*). No thermal event corresponding to the transformation of the low temperature form of Nb_2O_5 into its high temperature modification [8], α-Nb_2O_5, is observed in the DTA.

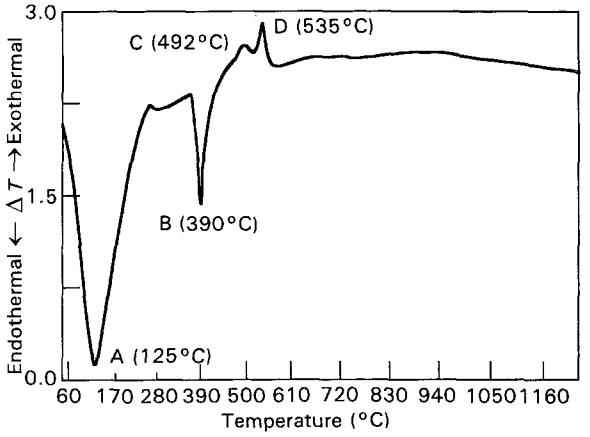

Figure 3 A typical DTA thermogram of the niobium pentoxide gel recorded at a scan rate of 10 °C min^{-1} in air. NB-2 gel; weight, 18 mg; atmosphere, air; scan rate 10 °C min^{-1}.

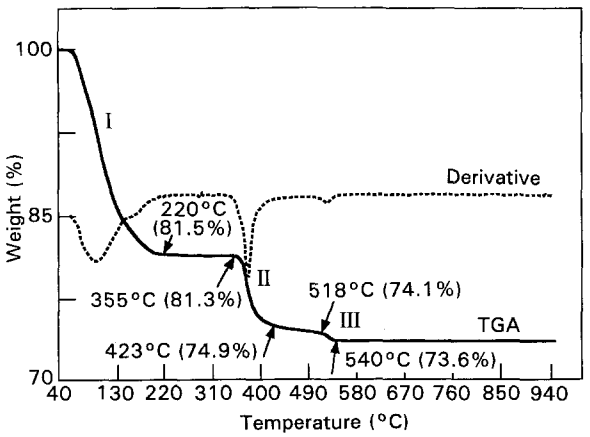

Figure 4 TGA curve and its derivative for the niobium pentoxide gel at a heating rate of 10 °C min^{-1} in air. NB-2 gel; weight, 20.6128 mg; atmosphere, air; scan rate, 10 °C min^{-1}.

3.5. Crystallization kinetics

A variable heating rate DSC method was used to evaluate the kinetics of crystallization of the amorphous niobium pentoxide. DSC scans were run at various heating rates between 1 and 40 K min^{-1}. A typical DSC thermogram recorded at a scan rate of 10 K min^{-1} is presented in Fig. 5. A sharp exothermic peak which may be assigned to crystallization of the amorphous material into niobium pentoxide is observed at 578 °C. The peak maximum temperatures at various heating rates are listed in Table III. The position of the exotherm shifted to higher temperature with increase in scan rate.

The kinetic model of Bansal and Doremus [9] was used to evaluate the values of the kinetic parameters from the DSC data. This model is expressed by the equation

$$\ln[T_p^2/\alpha] = \ln(E/R) - \ln\nu + E/(RT_p) \quad (3)$$

where T_p is the peak maximum temperature, α the heating rate, E the activation energy, R the gas constant, and ν the frequency factor. The crystallization kinetic parameters (E and ν) are related to the reaction rate constant, k, by an Arrhenius type expression

$$k = \nu\exp[-E/RT] \quad (4)$$

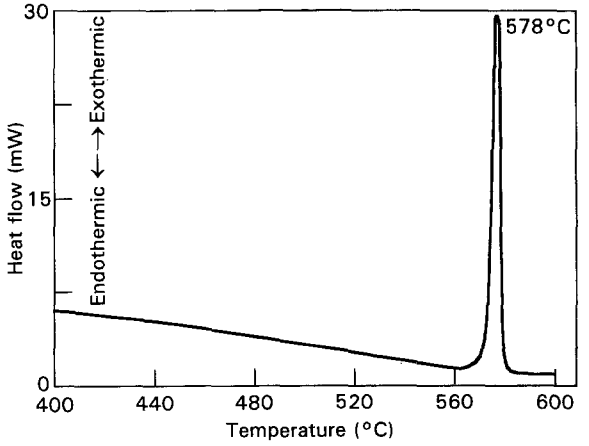

Figure 5 A typical DSC thermogram showing the crystallization peak for the niobium pentoxide gel calcined at 300 °C (24 h) and 400 °C (45 h), recorded at a heating rate of 10 °C min^{-1} in air. Sample weight, 6.17 mg.

TABLE III Effect of heating rate on the peak maximum temperature of the DSC exotherm for the crystallization of amorphous niobium pentoxide

Heating rate, α (K min^{-1})	Peak maximum temperature, T_p (K)	Heating rate, α (K min^{-1})	Peak maximum temperature, T_p (K)
1	818	10	852
2	828	15	853
2	832	15	860
5	838	20	860
5	841	30	868
10	851	40	871

Equation 3 is an extension of the Johnson–Mehl–Avrami [10] isothermal kinetic model for use in non-isothermal methods. In the derivation of Equation 3 it was assumed that the rate of reaction is maximum at the peak, which is a valid assumption for the power-compensated DSC. It has been demonstrated in earlier studies [9, 11–13] that the kinetic parameters determined from non-isothermal DSC using Equation 1 and from isothermal methods are in excellent agreement.

A plot of $\ln[T_p^2/\alpha]$ versus $1/T_p$ for the crystallization of amorphous niobium pentoxide prepared by the sol–gel technique was linear (Fig. 6) indicating the applicability of the kinetic model of Bansal and Doremus [9]. From linear least squares fitting, the values of the kinetic parameters were determined to be $E = 399\ \text{kJ mol}^{-1}$ and $\nu = 3.7 \times 10^{22}\ \text{s}^{-1}$, the correlation coefficient being 0.99.

3.6. I.r. spectroscopy

Infrared absorption spectra of the niobium pentoxide gel calcined at various temperatures were recorded between 450 to 4000 cm^{-1}. Typical results are presented in Fig. 7. Also shown for comparison is the spectra of the high temperature α-Nb_2O_5 phase obtained from a commercial source. The bands in the vicinity of 1650 and 3200 cm^{-1} are assigned to the absorptions due to water. The peak at $\sim 2280\ \text{cm}^{-1}$ is due to atmospheric carbon dioxide. As seen from XRD analysis, sample D is amorphous, F is the low temperature form, and K is the high temperature or α-modification of Nb_2O_5. The i.r. spectra of these three samples are quite distinct. The spectra of sample K is quite similar to that of the commercial α-Nb_2O_5. The peak at $\sim 835\ \text{cm}^{-1}$ may be attributed [14–19] to the Nb–O–Nb bonding parallel to the *b*-axis. The Nb–O–Nb bridging bond probably causes [14–19] the absorption band around 690 cm^{-1}, and the absorption peak at $\sim 500\ \text{cm}^{-1}$ may be assigned [14–19] to the ONb_3 structure.

It has been well established [20] by NMR spectroscopy that niobium pentaethoxide forms dimers which exist as the edge-shared octahedral structure as shown in Fig. 8. In this structure, each metal atom is bonded to two bridging and four terminal groups. The bridging Nb–O band and the terminal Nb–O band appear [21] at 485 and 575 cm^{-1}, respectively, and the bridging C–O band and the terminal C–O band appear [21] at 1030 and 1066 cm^{-1}, respectively.

Not many studies have been reported on the hydrolysis of niobium alkoxides. Yamaguchi *et al.* [22] synthesized a continuous series of solid solutions in

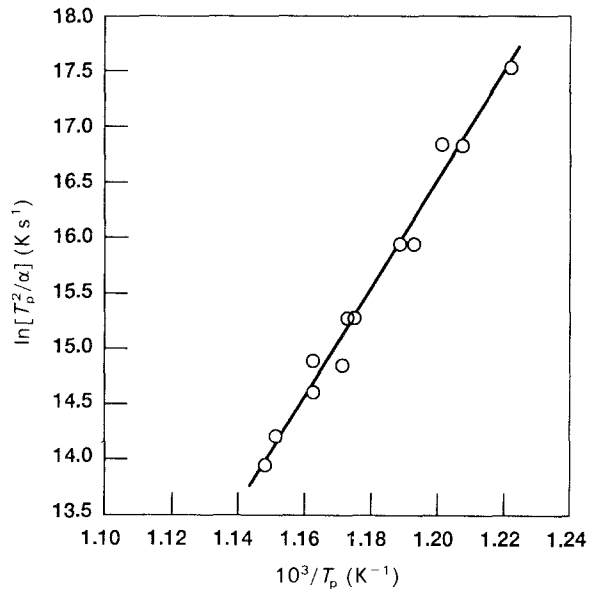

Figure 6 Plot of $\ln[T_p^2/^a]$ versus reciprocal of the DSC exothermic peak maximum temperature, T_p, for crystallization of the niobium pentoxide gel. Calcined at 300 °C (24 h) and 400 °C (45 h). $E = 399\ \text{kJ mol}^{-1}$, $\nu = 3.7 \times 10^{22}\ \text{s}^{-1}$, correlation coefficient = − 0.9907.

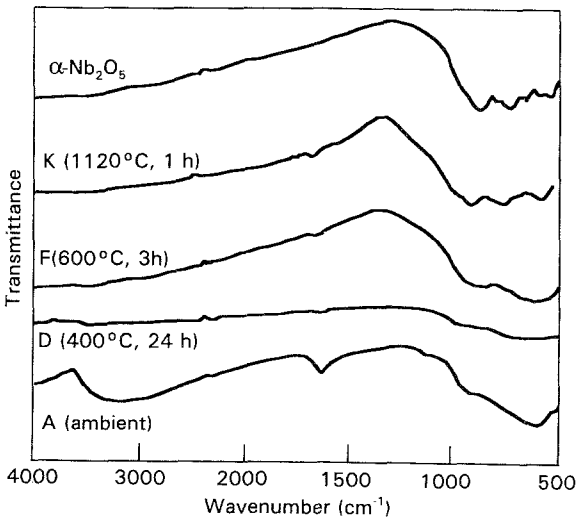

Figure 7 Infrared absorption spectra of niobium pentoxide gel calcined at different temperatures. For thermal histories of various samples refer to Table II.

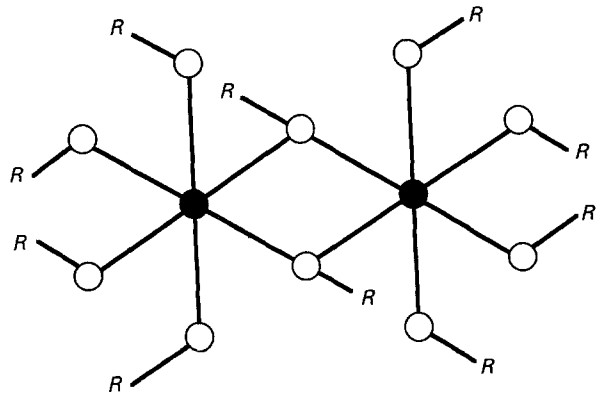

Figure 8 The structure of niobium pentaethoxide dimer where *R* represents the $-C_2H_5$ group: (●) Nb, (○) oxygen.

the Nb_2O_5–Ta_2O_5 system by the simultaneous hydrolysis of niobium and tantalum isopropoxides. Alquier *et al.* [6] have prepared niobium pentoxide gels using different approaches such as destabilization of a sol obtained by controlled hydrolysis of $NbCl_5$ with H_2O_2 and also by hydrolysis of $Nb(OC_2H_5)_5$ and niobium chloroalkoxides. The addition of H_2O_2 seemed to improve the process by removing chloride ions from the system through a redox reaction

$$3H_2O_2 + 2HCl \rightarrow 4H_2O + O_2 + Cl_2 \quad (5)$$

On hydrolysis of niobium pentaethoxide with tetramethylammonium hydroxide in methanol, decaniobate anion $Nb_{10}O_{28}^{6-}$ is formed [23]. Fuchs *et al.* [24] have reported the formation of various isopolyniobate ions, $Nb_6O_{19}^{6-}$, $Nb_{12}O_{37}^{14-}$, $Nb_{24}O_{65}^{10-}$ on hydrolysis of $Nb(OC_2H_5)_5$ with various organic bases at various water:Nb mole ratios. It is difficult to predict if such ionic species are present in our gels, which are produced without the presence of an organic base.

Alquier *et al.* [6] have carried out gelation of $Nb(OC_2H_5)_5$ using water:Nb mole ratio > 5.5. Due to the high reactivity of $Nb(OC_2H_5)_5$ with water, it was suggested that most probably the main reaction is

$$Nb(OC_2H_5)_5 + 5H_2O \rightarrow Nb(OH)_5 + 5C_2H_5OH \quad (6)$$

rather than

$$Nb(OC_2H_5)_5 + nH_2O \rightarrow Nb(OH)_n(OC_2H_5)_{5-n} + nC_2H_5OH \quad (7)$$

It was suggested that gelation must proceed through an olation–oxolation process between $Nb(OH)_5$ molecules with elimination of water, rather than polycondensation between hydroxoethoxy niobates with elimination of ethanol. A more detailed investigation is needed to decide whether Equation 6 or 7 is predominant.

4. Conclusions

Transparent monoliths and bulk powder of niobium pentoxide gels can be prepared from the hydrolysis of niobium pentaethoxide using hydrochloric acid as the deflocculating agent. The thermal evolution of physical and structural changes occurring in the gel were monitored by DTA, TGA, X-ray diffraction and infrared spectroscopy. The gels were amorphous to X-rays and crystallized into the low temperature form of Nb_2O_5 at $\sim 500\,^{\circ}C$, which transformed into the high temperature H- or α-Nb_2O_5 modification between 900 to 1000 °C. This transformation was irreversible, i.e. the α-Nb_2O_5 did not convert back into the low temperature form on cooling. The kinetics of crystallization of the amorphous powder were studied by non-isothermal DSC, and the crystallization activation energy was evaluated to be 399 kJ mol^{-1}. The results of the present study would be useful for applying a compliant/protective layer of niobium pentoxide on ceramic fibres for reinforcement of high temperature ceramic matrix composites because of the thermal and chemical stability of Nb_2O_5.

Acknowledgements

Thanks are due to Ralph Garlick for recording the powder X-ray diffraction patterns and to Beth Hyatt for her assistance with the thermal analyses and the infrared spectra.

References

1. S. SAKKA, *J. Non-Cryst. Solids* **100** (1988) 1.
2. B. REICHMAN and A. J. BARD, *J. Electrochem. Soc.* **128** (1981) 344.
3. N. KUMAGAI, K. TANNO, T. NAKAJIMA and N. WATANABE, *Electrochim Acta* **28** (1983) 17.
4. B. REICHMAN and A. J. BARD, *J. Electrochem. Soc.* **127** (1980) 241.
5. Y. Xi, H. McKINSTRY and L. E. CROSS, *J. Amer. Ceram. Soc.* **66** (1983) 637.
6. C. ALQUIER, M. T. VANDENBORRE and M. HENRY, *J. Non-Cryst. Solids* **79** (1986) 383.
7. J.C.P.D.S. Card No. 27–1003 (Powder Diffraction File, International Centre for Diffraction Data, Swarthmore, PA).
8. J.C.P.D.S. Card No. 16–53, (Powder Diffraction File, International Centre for Diffraction Data, Swarthmore, PA).
9. N. P. BANSAL and R. H. DOREMUS, *J. Thermal Anal.* **29** (1984) 115.
10. M. AVRAMI, *J. Chem. Phys.* **7** (1939) 1103.
11. N. P. BANSAL, R. H. DOREMUS, A. J. BRUCE and C. T. MOYNIHAN, *J. Amer. Ceram. Soc.* **66** (1983) 233.
12. N. P. BANSAL, A. J. BRUCE, R. H. DOREMUS and C. T. MOYNIHAN, *J. Non-Cryst. Solids* **70** (1985) 379.
13. *Idem., SPIE* **484** (1984) 51.
14. T. IKEYA and M. SENNA, *J. Non-Cryst. Solids* **105** (1988) 243.
15. V. BHIDE and E. HUSSON, *Mater. Res. Bull.* **15** (1980) 1339.
16. E. HUSSON, Y. REPELIN, N. Q. DAO and K. BRUSSET, *ibid.* **12** (1977) 1199.
17. G. T. STANFORD and R. A. CONDRATE, Sr, *J. Solid St. Chem.* **52** (1984) 248.
18. G. BLASSE and A. F. CONRSMIT, *ibid.* **10** (1974) 39.
19. A. A. McCONNEAL, J. S. ANDERSON and C. N. R. RAO, *Spectrochim. Acta.* **32A** (1976) 1067.
20. D. C. BRADLEY and C. E. HOLLOWAY, *J. Chem. Soc. A* (1968) 219.
21. D. C. BRADLEY, R. C. MEHROTRA and D. P. GAUR, "Metal Alkoxides" (Academic Press, London, 1978) pp. 116–122.
22. O. YAMAGUCHI, D. TOMIHISA, M. SHIRAI and K. SHIMIZU, *J. Amer. Ceram. Soc.* **71** (1988) C-260.
23. E. J. GRAEBER and B. MOROSIN, *Acta Cryst.* **B33** (1977) 2472.
24. J. FUCHS, K. F. JAHR and G. HELLER, *Chem. Ber.* **96** (1963) 2472.

Received 13 July 1993
and accepted 3 February 1994